

Photo-assisted Andreev reflection as a probe of quantum noise

Nguyen Thi Kim Thanh

*Centre de Physique Théorique, Case 907 Luminy, 13288 Marseille cedex 9, France
Université de la Méditerranée, 13288 Marseille Cedex 9, France and
Institute of Physics and Electronics, 10 Dao Tan, Cong Vi, Ba Dinh, Hanoi, Vietnam*

Adeline Crépieux

*Centre de Physique Théorique, Case 907 Luminy, 13288 Marseille cedex 9, France and
Université de la Méditerranée, 13288 Marseille Cedex 9, France*

Nguyen Ai Viet

Institute of Physics and Electronics, 10 Dao Tan, Cong Vi, Ba Dinh, Hanoi, Vietnam

Thierry Martin

*Centre de Physique Théorique, Case 907 Luminy, 13288 Marseille Cedex 9, France and
Université de la Méditerranée, 13288 Marseille cedex 9, France*

(Dated: May 24, 2019)

Andreev reflection, which corresponds to the tunneling of two electrons from a metallic lead to a superconductor lead as a Cooper pair (or vice versa), can be exploited to measure high frequency noise. A detector is proposed, which consists of a normal lead–quantum dot–superconductor circuit, which is capacitively coupled to a mesoscopic circuit where noise is to be measured. A substantial DC current can flow in the detector circuit only if an appropriate photon is provided or absorbed by the mesoscopic circuit, which plays the role of an environment for the dot–superconductor junction.

I. INTRODUCTION

Over the last decades, the measurement of noise has become a widely accepted diagnosis in the study of electronic quantum transport^{1,2,3}. Indeed, noise provides information on the charge of the carriers in unconventional conductor, when considering the Fano factor – the ratio of the noise to the average current – in the regime where the carriers tunnel independently. Away from this Poissonian regime, noise also contains crucial information on the statistics of the charge carriers⁴. Experimentally, low frequency “white” noise in the kHz–MHz range is more accessible than high frequency noise: it can in principle be measured using state of the art time acquisition techniques. For higher frequency measurements, it is becoming necessary to build a noise detector on chip for a specific range of high frequencies. In this work we consider a detector circuit which is capacitively coupled to the mesoscopic device. This circuit is composed of a normal lead, a quantum dot and a superconductor. Transport in this circuit occurs when the electrons tunneling between the dot and the superconductor are able to gain or to lose energy via photo-assisted Andreev reflections. The measurement of a DC current in the detector can thus provide information on the absorption and on the emission component of the current noise correlator.

More recently, theoretical efforts have been made to describe the high frequency noise measurement process⁵. This is motivated by the fact that in specific transport setups, high frequency noise detection is required in order to fully characterize transport. Examples are Bell inequality tests^{6,7} and the detection of the anomalous charges in one dimensional correlated systems^{8,9}. The former require information about high frequency noise in order to establish a correspondence between electron number correlators and current noise correlators. The latter requires a high frequency noise measurement in order to obtain a non-zero signal when the nanotube is connected to Fermi liquid leads.

In Ref. 10, a detection circuit, which was capacitively coupled to the mesoscopic circuit to be measured, was proposed as a high frequency noise detector. This idea was implemented experimentally recently^{11,12} using a superconductor-insulator-superconductor (SIS) junction for the detector circuit, and a Josephson junction for the sample to be measured. It was shown explicitly that the spectral density of noise, corresponding to absorption and emission between the two circuits, could be extracted from a DC measurement of the quasiparticle tunneling current in the on-chip measuring circuit. Very recently, the noise of a carbon nanotube/quantum dot was also measured¹³ using capacitive coupling to an SIS detector, with the detection of Super-Poissonian noise resulting from inelastic cotunneling processes.

The purpose of the present work is to analyze a similar situation, except that the SIS junction is replaced by a circuit which transfers two electrons via Andreev reflection. Andreev reflection¹⁴ typically assumes a good contact between a normal metal and a superconductor, but in general it can be applied to tunneling contacts – it can even

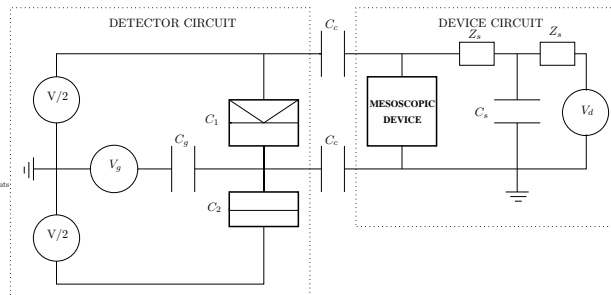


FIG. 1: Schematic description of the set up: the mesoscopic device to be measured is coupled capacitively to the detector circuit. The latter consists of a normal metal lead–quantum dot–superconductor circuit with a DC bias.

involve tunneling transitions via virtual states. In this work, Andreev reflection process occurs through a quantum dot, allowing to filter electron energies. Consequently, two successive inelastic electron jumps are required for a current to pass through the measurement circuit. Indeed, a DC measurement of this Andreev current can only occur if a “photon” with sufficient energy is emitted from or absorbed by the noise source – the circuit whose noise one wishes to characterize. The amplitude of the DC current as a function of bias voltage in the measurement circuit provides a readout of the noise power to be measured.

The detector circuit is depicted in Fig. 1. It consists of a normal metal lead, which is in good contact with a quantum dot operating in the Coulomb blockade regime. The charging energy of the dot is assumed to be large enough that double occupancy is prohibited. At the same time, the quantum dot is in tunneling contact with a superconductor. Below, we refer to this system as the normal metal–dot–superconductor (NDS) detector circuit. Two capacitors are placed, respectively, between each side of the mesoscopic device and each side of the quantum dot–superconductor tunnel junction. This means that a current fluctuation in the mesoscopic device generates, via the capacitors, a voltage fluctuation across the dot–superconductor tunnel junction. In turn, the voltage fluctuations translate into fluctuations of the phase around the junction. The presence of the neighboring mesoscopic circuit acts as a specific electromagnetic environment for this tunnel junction, which is described in the context of dynamical Coulomb blockade¹⁵ for this reason.

Fig. 2 discusses several scenarios for Andreev reflection. In the conventional picture of Andreev reflection¹⁴, two electrons tunnel on the normal side with exactly opposite energies with respect to the superconductor chemical potential (Fig. 2a). This implies that the chemical potential of the normal lead lies above that of the superconductor. Next, one considers the case where a quantum dot is inserted in the path between the normal metal lead and the superconductor (Fig. 2b). The quantum dot level is located above the superconductor chemical potential. In the case where double occupancy is prohibited by the Coulomb blockade, Andreev transport occurs via sequential tunneling of the two electrons. Yet, because of energy conservation, the same energy requirements as in Fig. 2a have to be satisfied for the final states (electrons with opposite energies). In T-matrix terminology, for this transition to occur, virtual states corresponding to the energy of the dot are required, which suppress the Andreev tunneling current because of large energy denominators in the transition rate. Fig. 2 c, d, e, describe the cases where an environment is coupled to the same NDS circuit. Provided that this environment can yield some of its energy to the NDS detector, electronic transitions via the dot can become much more likely. In particular, these transitions can occur even of the chemical potential of the normal lead exceeds that of the superconductor. As we shall see later on, the bias voltage can act as a valve for photo-assisted electron transitions. It is precisely these latter situations which will be used to measure the noise of the measuring circuit (the “environment”).

The paper is organized in the following way: we present the model in Sec. II, the calculation of the photo-assisted current is given in Sec. III. Next, in Sec. IV, we apply our result in the case of a quantum point contact and discuss the effects of the detector bias voltage, device bias voltage and dot level position.

II. MODEL HAMILTONIAN

The Hamiltonian which describes the decoupled normal metal lead–dot–superconductor–environment (mesoscopic circuit) system reads

$$H_0 = H_{0L} + H_{0D} + H_{0S} + H_{env} , \quad (1)$$

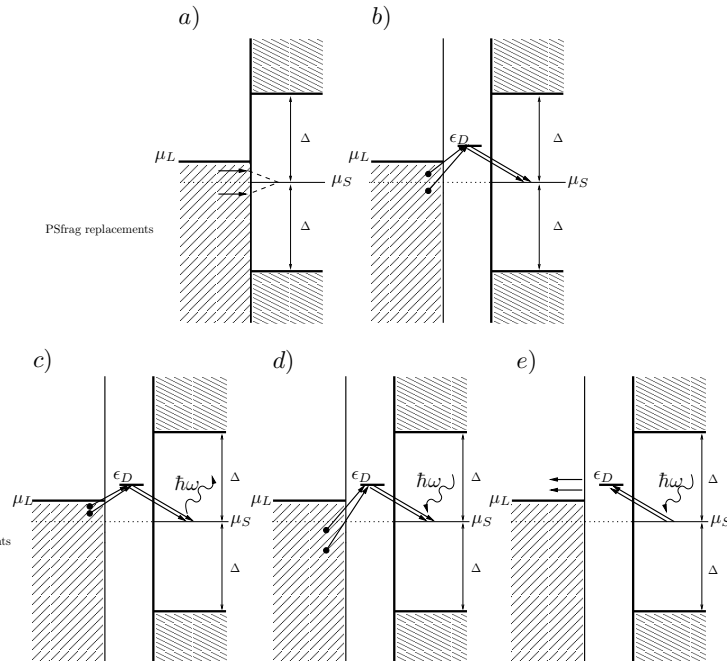


FIG. 2: Andreev reflection: emission (a,b,c,d) and absorption (e) of a Cooper pair in a normal metal. a) Case of a normal metal–superconducting junction. b) Case of an NDS junction operating in the elastic regime. c), d) Case of photo-assisted Andreev reflection, where a “photon” is provided to or provided by a neighboring environment. e) Case of absorption of a Cooper pair with photo-assisted Andreev reflection, where a “photon” is provided by a neighboring environment. For case c), d), e), which require passing through the dot, the tunneling of electrons is sequential.

where

$$H_{0L} = \sum_{k,\sigma} \epsilon_k c_{k,\sigma}^+ c_{k,\sigma} , \quad (2)$$

describes the energy states in the lead. The Hamiltonian for the quantum dot reads

$$H_{0D} = \sum_{\sigma} \epsilon_D c_{D,\sigma}^+ c_{D,\sigma} + U n_{\uparrow} n_{\downarrow} , \quad (3)$$

where U will be assumed to be infinite, assuming a small capacitance of the dot. We consider that the dot possesses only a single energy level for simplicity. The diagonalized superconductor Hamiltonian takes the form

$$H_{0S} - \mu_S N_S = \sum_{q,\sigma} E_q \gamma_{q,\sigma}^+ \gamma_{q,\sigma} , \quad (4)$$

where $\gamma_{q,\sigma}, \gamma_{q,\sigma}^+$ are quasiparticle operators, which relate to the Fermi operators $c_{q,\sigma}, c_{q,\sigma}^+$ by the Bogoliubov transformation

$$\begin{aligned} c_{-q,\downarrow} &= u_q \gamma_{-q,\downarrow} - v_q \gamma_{q,\uparrow}^+ , \\ c_{q,\uparrow}^+ &= u_q \gamma_{q,\uparrow}^+ + v_q \gamma_{-q,\downarrow} , \end{aligned} \quad (5)$$

and $E_q = \sqrt{\Delta^2 + \zeta_q^2}$ is the quasiparticle energy, $\zeta_q = \epsilon_q - \mu_S$ is the normal state single-electron energy counted from the Fermi level μ_S , Δ is the superconducting gap, which will be assumed to be the largest energy scale in these calculations.

Here we do not specify the Hamiltonian of the environment because the environment represents an open system: the mesoscopic circuit which represents the environment will only manifest itself via the phase fluctuations $\langle\phi(0)\phi(t)\rangle$ which are induced in the NDS circuit, at the dot–superconductor junction because of the location of the capacitor plates. In what follows, we shall assume that the unsymmetrized noise spectral density

$$S^+(\omega) = \int \frac{dt}{2\pi} e^{i\omega t} \langle\langle I(0)I(t)\rangle\rangle , \quad (6)$$

corresponding to emission (for positive frequency), or alternatively $S^-(\omega) \equiv S^+(-\omega)$, the spectral density of noise corresponding to absorption, are both specified by the transport properties of the mesoscopic circuit^{5,16,17}. Here $\langle\langle \dots \rangle\rangle$ stands for an irreducible noise correlator, where the product of average currents has been subtracted out.

The tunneling Hamiltonian includes electron transferring between the superconductor and the dot, as well as the tunneling between the dot and the normal metal lead

$$\begin{aligned} H_T &= (H_{T1} + H_{T2}) + h.c. , \\ H_{T1} &= \sum_{q,\sigma} T_{D,q} c_{D,\sigma}^+ c_{q,\sigma} e^{-i\phi} , \\ H_{T2} &= \sum_{k,\sigma} T_{k,D} c_{k,\sigma}^+ c_{D,\sigma} , \end{aligned} \quad (7)$$

the index k, D, q refer to the normal metal lead (L), quantum dot (QD) superconductor (S). We consider the simple case $T_{D,q} = T_1$, $T_{k,D} = T_2$, assuming a constant normal metal density of states on both sides of the dot. Note that H_{T1} contains a fluctuating phase factor, which represents the coupling to the mesoscopic circuit. Indeed, because of the capacitive coupling between the sides of the dot–superconductor junction and the mesoscopic circuit, a current fluctuation translates into a voltage fluctuation across the dot–superconductor junction. They are related via a trans-impedance¹⁰. Next, the voltage fluctuations translate into phase fluctuations across the junction, as the phase is the canonical conjugate of the charge at the junctions¹⁵: the phase is thus considered as a quantum mechanical operator throughout this paper.

The present system bears similarities with the study of inelastic Andreev reflection in the case where the superconductor contains phase fluctuations^{18,19}. Such phase fluctuations destroy the symmetry between electrons and holes, and affect the current voltage characteristics of the NS junction.

III. TUNNELING CURRENT

The tunneling current associated with two electrons is given by the Fermi Golden Rule $I = 2e\Gamma_{i\rightarrow f}$, with the tunneling rate

$$\Gamma_{i\rightarrow f} = 2\pi \sum_f |\langle f|T|i\rangle|^2 \delta(\epsilon_i - \epsilon_f) , \quad (8)$$

where ϵ_i and ϵ_f are the tunneling energies of the initial and final states, including the environment, T is the transition operator, which is expressed as

$$T = H_T + H_T \sum_{n=1}^{\infty} \left(\frac{1}{i\eta - H_0 + \epsilon_i} H_T \right)^n , \quad (9)$$

with η is a positive infinitesimal.

Here one needs to carry out calculations of the matrix element in Eq. (8) to fourth order in the tunneling Hamiltonian. Indeed, there are two possibilities: a Cooper pair in the superconductor is transmitted to the normal lead or vice versa. The first process involves the electron from a Cooper pair tunneling onto the dot, next this electron escapes in the lead. The other electron from the same Cooper pair undergoes the same two tunneling processes. Similar transitions, in the opposite direction, are necessary for two electrons from the normal lead to end up as a Cooper pair in the superconductor. Note that this description of events assumes implicitly that S remains in the ground state in the initial and final states. On the other hand, if L is initially in the ground state (filled Fermi sea), it is left in an excited state with two electrons having energies above Fermi energy E_F in the final state. The extra energy has been provided by the environment. Typically,

$$|i\rangle = |G_L\rangle \otimes |G_S\rangle \otimes |0_{QD}\rangle \otimes |R\rangle , \quad (10)$$

where $|G\dots\rangle$ denotes a ground state, which corresponds to a filled Fermi sea for the normal electrode. $|0_{QD}\rangle$ is the vacuum of the quantum dot, and $|R\rangle$ denotes the initial state of the environment. On the other hand our guess for the final state should read

$$|f\rangle = 2^{-1/2}[c_{k,\sigma}^+ c_{k',-\sigma}^+ - c_{k',\sigma}^+ c_{k,-\sigma}^+]|G_L\rangle \otimes |G_S\rangle \otimes |0_{QD}\rangle \otimes |R'\rangle, \quad (11)$$

when a Cooper pair is emitted from S, or

$$|f\rangle = 2^{-1/2}[c_{k,\sigma} c_{k',-\sigma} - c_{k',\sigma} c_{k,-\sigma}]|G_L\rangle \otimes |G_S\rangle \otimes |0_{QD}\rangle \otimes |R'\rangle, \quad (12)$$

when S absorbs a Cooper pair. Here, $|R'\rangle$ the final state of the environment. The ‘‘guess’’ of Eqs. (11) and (12) is an informed one: indeed, the s-wave symmetry of the superconductor imposes that only singlet pairs of electrons can be emitted or absorbed. This phenomenon has been described in the early work on entanglement in mesoscopic physics^{20,21}, and the resulting final state can in principle be detected through a violation of Bell inequalities⁶.

Introducing the closure relation for the eigenstates of the non-connected system $\{|v_i\rangle\}$, and using the fact that $\langle v|(\epsilon_i - H_0 \pm i\eta)^{-1}|v\rangle = \mp i \int_0^\infty dt e^{i(\epsilon_i - \epsilon_v \pm i\eta)t}$, one can exponentiate all the energy denominators. Then, by transforming the time dependent phases into a time dependence of the tunneling Hamiltonian, we can integrate out all final and virtual states. This allows to rewrite the tunneling current in terms of tunneling operators in the interaction representation, to lowest order $O(T_1^4 T_2^4)$.

For the case of two electrons tunnel from S to L, the current reads

$$\begin{aligned} I_{\leftarrow} &= 2e \int_{-\infty}^{\infty} dt \int_0^{\infty} dt_1 \int_0^{\infty} dt_2 \int_0^{\infty} dt_3 \int_0^{\infty} dt'_1 \int_0^{\infty} dt'_2 \int_0^{\infty} dt'_3 e^{-\eta(t_1+t_2+t_3+t'_1+t'_2+t'_3)} \\ &\quad \times e^{-i(\mu_D - \mu_S)(2t-t'_1-t'_2-2t'_3+t_1+t_2+2t_3)} e^{-i(\mu_L - \mu_D)(2t-t'_2-t'_3+t_2+t_3)} \\ &\quad \times \langle H_{T1}^+(t-t'_1-t'_2-t'_3+t_1+t_2+t_3) H_{T2}^+(t-t'_2-t'_3+t_1+t_2+t_3) H_{T1}^+(t-t'_3+t_1+t_2+t_3) H_{T2}^+(t+t_1+t_2+t_3) \\ &\quad \times H_{T2}(t_1+t_2+t_3) H_{T1}(t_1+t_2) H_{T2}(t_1) H_{T1}(0) \rangle. \end{aligned} \quad (13)$$

For the case of two electrons tunnel from L to S, the current is

$$\begin{aligned} I_{\rightarrow} &= 2e \int_{-\infty}^{\infty} dt \int_0^{\infty} dt_1 \int_0^{\infty} dt_2 \int_0^{\infty} dt_3 \int_0^{\infty} dt'_1 \int_0^{\infty} dt'_2 \int_0^{\infty} dt'_3 e^{-\eta(t_1+t_2+t_3+t'_1+t'_2+t'_3)} \\ &\quad \times e^{-i(\mu_D - \mu_L)(2t-t'_1-t'_2-2t'_3+t_1+t_2+2t_3)} e^{-i(\mu_S - \mu_D)(2t-t'_2-t'_3+t_2+t_3)} \\ &\quad \times \langle H_{T2}(t-t'_1-t'_2-t'_3+t_1+t_2+t_3) H_{T1}(t-t'_2-t'_3+t_1+t_2+t_3) H_{T2}(t-t'_3+t_1+t_2+t_3) H_{T1}(t+t_1+t_2+t_3) \\ &\quad \times H_{T1}^+(t_1+t_2+t_3) H_{T2}^+(t_1+t_2) H_{T1}^+(t_1) H_{T2}^+(0) \rangle. \end{aligned} \quad (14)$$

First, we calculate I_{\leftarrow} . The same method is applied to calculate I_{\rightarrow} . The problem is thus reduced to the calculation of correlators of the tunneling Hamiltonian in the ground state. Using Wick’s theorem, these can be expressed in terms of single particle Green’s function because the Hamiltonian of the isolated components is quadratic (except, maybe for the environment, which is dealt separately). These cumbersome calculations are presented in the Appendix A: the correlators contains averages of fermion operators, as well as averages of exponentiated phases $e^{i\phi(t)}$. The latter can be computed easily if all times in the exponential are ordered, for instance as it was achieved in Ref. 22 for noise correlations in Luttinger liquids. For definition purposes, it is convenient to introduce the correlation of the phase operators

$$J(t) = \langle [\phi(t) - \phi(0)]\phi(0) \rangle, \quad (15)$$

where the phase operator is related to the voltage by the relation

$$\phi(t) = e \int_{-\infty}^t dt' V(t'). \quad (16)$$

Given a specific circuit (capacitors, resistances,...) the trans-impedance relates the voltage fluctuations across the superconductor-quantum dot junction to the current fluctuation of the mesoscopic circuit to be measured: $V(\omega) = Z(\omega)I(\omega)$. The phase correlator is therefore expressed in terms of the trans-impedance of the circuit and the spectral density of noise¹⁰

$$J(t) = \frac{2\pi}{R_K} \int_{-\infty}^{\infty} d\omega \frac{|Z(\omega)|^2}{\omega^2} S_I(\omega) (e^{-i\omega t} - 1), \quad (17)$$

where $R_K = 2\pi/e^2$ is the quantum of resistance and $S_I(\omega) = S^+(-\omega)$.

We can now write the tunneling current as a function of the normal (and anomalous) Green's functions of the normal metal lead, $G_{L\sigma}(t)$, the quantum dot, $G_{D\sigma}(t)$, and the superconductor, $F_\sigma(t)$ (see Appendix A)

$$\begin{aligned}
I_{\leftarrow} = & 2eT_1^4T_2^4 \int_{-\infty}^{\infty} dt \int_0^{\infty} dt_1 \int_0^{\infty} dt_2 \int_0^{\infty} dt_3 \int_0^{\infty} dt'_1 \int_0^{\infty} dt'_2 \int_0^{\infty} dt'_3 e^{-\eta(t_1+t_2+t_3+t'_1+t'_2+t'_3)} \\
& \times e^{-i(\mu_D-\mu_S)(2t-t'_1-t'_2-2t'_3+t_1+t_2+2t_3)} e^{-i(\mu_L-\mu_D)(2t-t'_2-t'_3+t_2+t_3)} \\
& \times \sum_{\sigma} \left[-F_{\sigma}^*(t'_1+t'_2)F_{-\sigma}(t_1+t_2)G_{L\sigma}(t-t'_2-t'_3)G_{L-\sigma}(t+t_2+t_3)G_{D\sigma}(-t'_1)G_{D-\sigma}(-t'_3)G_{D\sigma}(t_3)G_{D-\sigma}(t_1) \right. \\
& \left. +F_{\sigma}^*(t'_1+t'_2)F_{\sigma}(t_1+t_2)G_{L\sigma}(t-t'_2-t'_3+t_2+t_3)G_{L-\sigma}(t)G_{D\sigma}(-t'_1)G_{D-\sigma}(-t'_3)G_{D-\sigma}(t_3)G_{D\sigma}(t_1) \right] \\
& \times e^{J(t-t'_1-t'_2-t'_3+t_1+t_2+t_3)+J(t-t'_3+t_1+t_2+t_3)+J(t-t'_1-t'_2-t'_3+t_3)+J(t-t'_3+t_3)-J(-t'_1-t'_2)-J(t_1+t_2)} .
\end{aligned} \tag{18}$$

Using the assumption $\mu_S = 0$, we further assume that $J(t) \ll 1$, which means a low trans-impedance approximation together with the fact that $J(t)$ is well behaved at large times. This allows to expand the exponential of phase correlators.

The result for the current contains both an elastic and an inelastic contribution as in Ref. 10. Since $\epsilon_k, \epsilon_{k'} \subset [eV, +\infty)$, with $eV > 0$, only an inelastic current is allowed

$$I_{\leftarrow} \simeq \frac{16\pi^2e}{R_K} \mathcal{N}_N^4 T_1^4 T_2^4 \int_{eV}^{\infty} d\epsilon \int_{eV}^{\infty} d\epsilon' \int_{\Delta}^{\infty} dE \int_{\Delta}^{\infty} dE' \frac{\Delta^2}{\sqrt{E^2 - \Delta^2} \sqrt{E'^2 - \Delta^2}} \frac{|Z(-(\epsilon + \epsilon'))|^2}{(\epsilon + \epsilon')^2} \frac{S_I(-(\epsilon + \epsilon'))}{D^{inel}} , \tag{19}$$

where D^{inel} is the denominator product attributed to the inelastic current, which is defined in Eq. (35) of Appendix B.

In the same way, we calculate I_{\rightarrow} , with the condition $\epsilon_k, \epsilon_{k'} \subset (-\infty, eV]$, $eV > 0$. This time, the current has both an elastic and an inelastic contribution

$$I_{\rightarrow} = I_{\rightarrow}^{el} + I_{\rightarrow}^{inel} , \tag{20}$$

where the elastic contribution is

$$\begin{aligned}
I_{\rightarrow}^{el} \simeq & 8\pi e \mathcal{N}_N^4 T_1^4 T_2^4 \int_{-eV}^{eV} d\epsilon \int_{\Delta}^{\infty} dE \int_{\Delta}^{\infty} dE' \frac{\Delta^2}{\sqrt{E^2 - \Delta^2} \sqrt{E'^2 - \Delta^2}} \left\{ \left[1 - \frac{4\pi}{R_K} \int_{-\infty}^{+\infty} d\omega \frac{|Z(\omega)|^2}{(\omega)^2} S_I(\omega) \right] \frac{1}{D^0} \right. \\
& \left. - \frac{2\pi}{R_K} \int_{-\infty}^{+\infty} d\omega \frac{|Z(\omega)|^2}{(\omega)^2} \frac{S_I(\omega)}{D^{el}} \right\} ,
\end{aligned} \tag{21}$$

with D^0 is the original denominator which is not affected by the environment, which is defined by Eq. (33) and D^{el} is the denominator product affected by the environment (see Eq. (34) of Appendix B). The inelastic contribution to I_{\rightarrow} is

$$I_{\rightarrow}^{inel} \simeq \frac{16\pi^2e}{R_K} \mathcal{N}_N^4 T_1^4 T_2^4 \int_{-\infty}^{eV} d\epsilon \int_{-\infty}^{eV} d\epsilon' \int_{\Delta}^{\infty} dE \int_{\Delta}^{\infty} dE' \frac{\Delta^2}{\sqrt{E^2 - \Delta^2} \sqrt{E'^2 - \Delta^2}} \frac{|Z(\epsilon + \epsilon')|^2}{(\epsilon + \epsilon')^2} \frac{S_I(\epsilon + \epsilon')}{D^{inel}} . \tag{22}$$

The I_{\rightarrow}^{el} term describes the elastic current while environment affects to the detector system or not. If $\omega \ll E, E'$, both of them reduce to the case there is no effect of the environment in the elastic part. Later on, with our study, we do not consider this term in our calculations. All contributions to the current contain denominators where the infinitesimal η (adiabatic switching parameter) is included in order to avoid divergencies. In fact, it has been shown in Ref. 20,23,24 that a proper resummation of the perturbation series, including all round trips from the dot to the normal leads, has the simple effect of replacing η by $\pi|T_2^2|\mathcal{N}_N$. In what follows, for simplicity we keep η in our expressions, bearing in mind that it represents the line width associated with the normal lead. For numerical purposes, it will be sufficient to assume that η is kept very small compared to the superconducting gap, as well as all the relevant level spacings (dot level position, bias voltages, etc...). The total current for tunneling of electrons through the NDS junction is therefore

$$I = I_{\rightarrow} - I_{\leftarrow} .$$

The above expressions constitute the central result of this work: one understands now how the current fluctuations in the neighboring mesoscopic circuit give rise to inelastic and elastic contributions in the current.

IV. QUANTUM POINT CONTACT AS A SOURCE OF NOISE

In this section, we illustrate the present results with a simple example. We consider for this purpose a quantum point contact, which is a device whose noise spectral density is well characterized

$$S^+(\omega) = \begin{cases} \frac{2e^2}{\pi} T(1-T)(eV_d - \hbar\omega)\theta(eV_d - \hbar\omega), & \text{if } \omega \geq 0, \\ \frac{2e^2}{\pi} [-2T^2\hbar\omega - T(1-T)(eV_d + \hbar\omega)\theta(-eV_d - \hbar\omega) + T(1-T)(eV_d - \hbar\omega)], & \text{if } \omega < 0, \end{cases} \quad (23)$$

where $\theta(x)$ is the Heaviside function and T is the transmission probability.

We can calculate directly the PAT current using this spectral density of noise. However, experimentally¹² it is difficult to distinguish unambiguously between symmetrized and non-symmetrized noise, partly because what is often measured is the excess noise, i.e. the difference between current fluctuations at a given bias and zero bias. We thus consider the measurement of excess noise from the mesoscopic device and with the detection scheme described here: we can show the interplay of absorption and emission processes between the two circuits. The spectral density of excess noise bears most of its weight near zero frequencies, but the noise decreases linearly to zero over a range $[0, \pm eV_d]$ for positive and negative frequencies

$$S_{\text{excess}}^+(\omega) = (2e^2/\pi)T(1-T)(eV_d - |\hbar\omega|)\theta(eV_d - |\hbar\omega|), \quad (24)$$

In this work, we thus measure the photon assisted tunneling (PAT) current through the detector due to the high frequency current fluctuations of the device, as a function of detector bias voltage

$$I_{PAT}(eV) = I(eV_d \neq 0, eV) - I(eV_d = 0, eV). \quad (25)$$

If we consider $eV_d < \Delta/2$, $\epsilon_D, eV \ll \Delta$ then, like in Ref. 25, we can approximate the quasiparticle energies in the denominators as follows $[E' + \epsilon_x + i\eta]^{-1} \simeq E'^{-1}$, $[E + \epsilon_x - i\eta]^{-1} \simeq E^{-1}$, where $\epsilon_x = \epsilon_D, \pm\epsilon', \pm\epsilon$, or $\epsilon_D - (\epsilon + \epsilon')$.

Considering the circuit in Fig. 1, at $\omega = 0$, device and detector are not coupled. The transimpedance is predicted to have a constant behavior at large frequency. We therefore choose the following form for transimpedance

$$|Z(\omega)|^2 = \frac{(R\omega)^2}{\omega_0^2 + \omega^2}, \quad (26)$$

where R is the typical high frequency impedance and ω_0 is estimated from the experimental data of Ref. 12, choosing a finite ω_0 means that at low frequencies $\omega < \omega_0$, the mesoscopic circuit has no influence on the detector circuit because low frequencies do not propagate through a capacitor.

The PAT current is thus computed in units of $(2)^7 \pi e^3 T(1-T) \mathcal{N}_N^4 T_1^4 T_2^4 R^2 / \Delta^2 R_K$,

$$\begin{aligned} I_{PAT} \simeq & \int_{-eV_d}^0 d\epsilon \int_{-eV_d}^0 d\epsilon' \frac{eV_d + \epsilon + \epsilon'}{\omega_0^2 + (\epsilon + \epsilon')^2} \theta(-\epsilon - \epsilon') \theta(eV_d + \epsilon + \epsilon') \frac{1}{\epsilon - \epsilon_D - i\eta} \left[\frac{1}{\epsilon - \epsilon_D + i\eta} + \frac{1}{\epsilon' - \epsilon_D + i\eta} \right] \\ & + \int_0^{eV} d\epsilon \int_0^{eV} d\epsilon' \frac{eV_d - \epsilon - \epsilon'}{\omega_0^2 + (\epsilon + \epsilon')^2} \theta(\epsilon + \epsilon') \theta(eV_d - \epsilon - \epsilon') \frac{1}{\epsilon - \epsilon_D - i\eta} \left[\frac{1}{\epsilon - \epsilon_D + i\eta} + \frac{1}{\epsilon' - \epsilon_D + i\eta} \right] \\ & - \int_{eV}^{eV_d - eV} d\epsilon \int_{eV}^{eV_d - eV} d\epsilon' \frac{eV_d - \epsilon - \epsilon'}{\omega_0^2 + (\epsilon + \epsilon')^2} \theta(eV_d - \epsilon - \epsilon') \frac{1}{\epsilon - \epsilon_D - i\eta} \left[\frac{1}{\epsilon - \epsilon_D + i\eta} + \frac{1}{\epsilon' - \epsilon_D + i\eta} \right]. \quad (27) \end{aligned}$$

The first two terms describe the tunneling of a Cooper pair from the normal lead to the superconductor via the quantum dot. The electrons can absorb energy (first term, corresponding to the $I_{\rightarrow}^{\text{absorb}}$ contribution in photo-assisted current) or emit energy (second term, corresponding to the $I_{\rightarrow}^{\text{emit}}$ contribution). The last term describes the inverse tunneling process: a Cooper pair absorbing energy from the neighboring device, its constituent electrons then tunneling from the superconductor to the normal lead (corresponding to the I_{\leftarrow} contribution). Our calculation applies to the zero temperature case. The energy scale is fixed by the superconductor gap ($\Delta = 1$), the appropriate parameters are chosen fixed: $\omega_0 = 0.01$, $\eta = 0.001$.

We easily see that the $I_{\rightarrow}^{\text{absorb}}$ contribution does not depend on the detector bias voltage eV , the $I_{\rightarrow}^{\text{emit}}$ contribution depends on eV if $eV < eV_d$, while the I_{\leftarrow} contribution is nonzero if $eV_d > 2eV$. At $eV \ll \epsilon_D$, only the I_{\leftarrow} contributes to the current (that means we do not take a constant $I_{\rightarrow}^{\text{absorb}}$). Increasing eV , but keeping eV still smaller than ϵ_D , there is a competition between the two current $I_{\rightarrow}^{\text{emit}}$ and I_{\leftarrow} . Then, when $eV > \epsilon_D$, only the $I_{\rightarrow}^{\text{emit}}$ contributes to the current. These effects are shown in the plots.

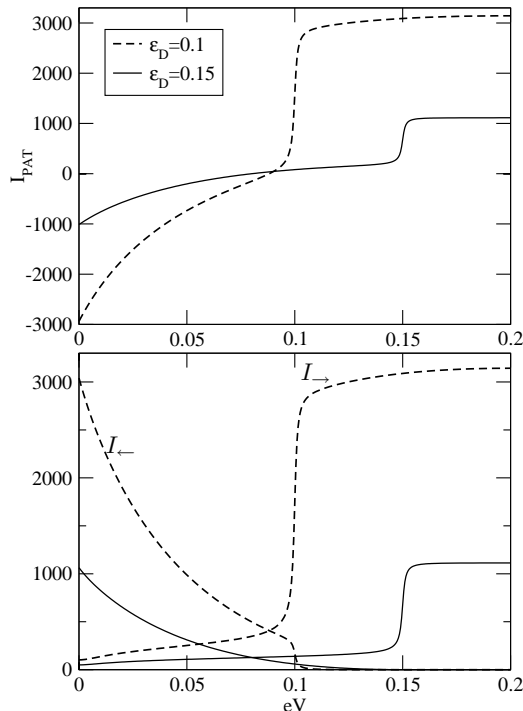


FIG. 3: PAT current (panel above), I_{\leftarrow} , and I_{\rightarrow} (panel lower) depending on bias voltage of detector with some values of dot energy level: 0.1 (dashed line), 0.15 (continuous line), and $eV_d = 0.3$.

Fig. 3 displays the PAT current as a function of bias voltage for different values of the dot position (panel above). The voltage imposed on the mesoscopic circuit is larger than the dot level position, which implies that photo-assisted transitions of electrons are possible. Understandingly, the current rises from negative values at $eV = 0$, but next it reaches a step, which height depends crucially on the dot level position: the step occurs when $eV = \epsilon_D$. When this step is reached, inelastic transitions from the normal lead to the superconductor are favored: the electrons no longer need to go through virtual states far in energy, in order to reach the superconductor, as they use the resonant level ϵ_D . Nevertheless, pairs of such electrons need to lose an energy of the order $2\epsilon_D$ in order to form a Cooper pair. For illustrative purposes, we have plotted the absolute magnitude of I_{\rightarrow} and I_{\leftarrow} on the lower panel. When considering electrons emitted from the superconductor to the normal lead, when $\epsilon_D < eV_d/2$, we also notice a step in this current. This time electrons from the superconductor need to gain energy from the environment in order to reach the dot and lead. However, such a transition can not occur if the final electron states are already occupied. This explains why the current becomes noticeable when $eV < \epsilon_D$.

Fig. 4 provides more details of the current curves and displays the case $\epsilon_D < eV_d/2$ (left panel), as well as the case $\epsilon_D > eV_d/2$ (right panel). Notice from Fig. 4 that the PAT current contribution for electrons tunneling from the normal lead to the superconductor by absorbing energy from the device circuit (process of Fig. 2d) is independent of eV ; it is a (small) constant and it can be neglected in front of the other (emission) contribution (process of Fig. 2c) when $eV > \epsilon_D$. So, the shape of I_{\rightarrow} is determined by the PAT current contribution of electron tunneling from the normal lead to the superconductor by emitting energy to the mesoscopic device. In the left panel, the steps of both I_{\leftarrow} and I_{\rightarrow}^{emit} happen at $eV = \epsilon_D$, but in the right panel, I_{\leftarrow} does not display any significant step, this current part approaches zero before $eV = \epsilon_D$, while the step of I_{\rightarrow} still happens at $eV = \epsilon_D$. The current-voltage characteristic demonstrates well the photo-assisted electron tunneling processes, from these curves we “detect” quantitatively the current fluctuations in the device system, specially we recognize the absorption and emission processes of the mesoscopic device. Note also that the scales for the currents in the two panels are quite different: the lower the dot energy level, the more electron transitions are favored because less energy needs to be supplied or extracted by the mesoscopic device.

Fig. 5 depicts the PAT current as a function of detector bias voltage for a fixed dot energy level position, but for different values of the device bias eV_d . We find that when the bias of the mesoscopic device increases, the current fluctuations increase, energy emitted or absorbed also increases, which in turn increases the PAT current (both the step at $eV = \epsilon_D$ and the amplitude of current at eV close to 0, increase with eV_d). From $eV_d = \epsilon_D$, if we decrease eV_d ,

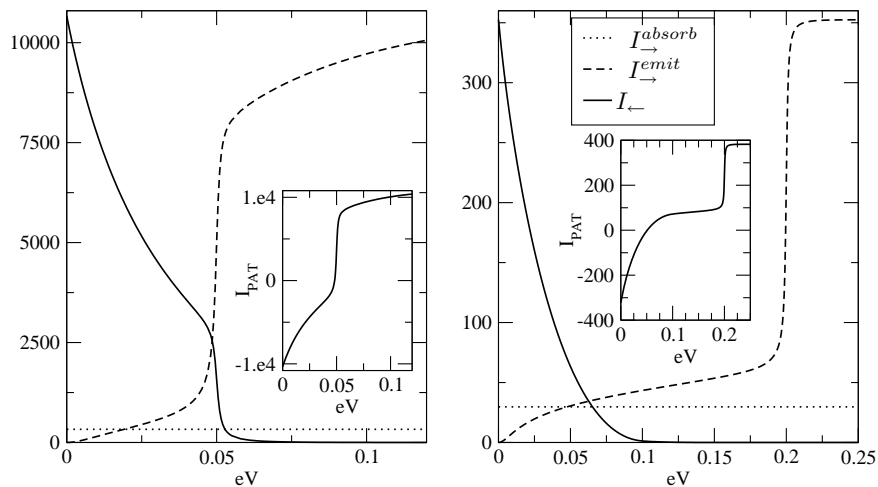


FIG. 4: Contribution of I_{\rightarrow} for which energy is absorbed from the environment (dotted line), contribution of I_{\rightarrow} for which energy is emitted to the environment (dashed line), I_{\leftarrow} (continuous line), as a function of bias voltage. The PAT current is plotted in the insert. Here, we ct

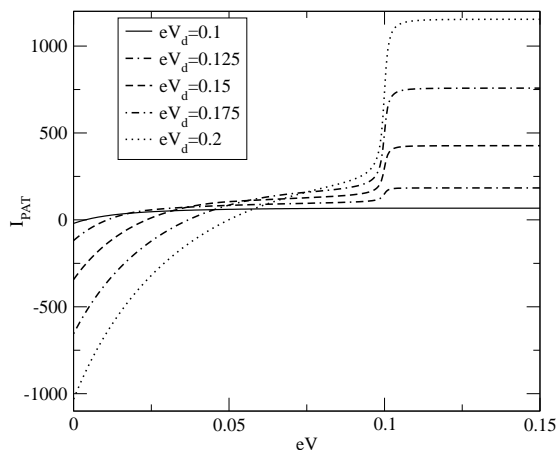


FIG. 5: PAT current plotted as a function of detector bias voltage for some values of the device bias voltage eV_d from 0.1 to 0.2 (see legend), with $\epsilon_D = 0.1$.

the PAT current is reduced, approaching 0 and the step disappears hereafter. This is realized at the point when the spectral density of noise of the mesoscopic device (point contact) contains a singularity in its derivative, $\epsilon_D \geq eV_d$, there is not more available noise: there is no energy emitted to or absorbed by the NDS junction.

In Fig. 6 we plot the dependence of the PAT current on the dot energy level for several values of the bias voltage of the detector circuit, which is chosen smaller than the (fixed) device bias voltage $eV_d = 0.2$, specifying $eV > eV_d/2$. By choosing this range of eV , only I_{\rightarrow} contributes to the current, according to Eq. (27). In this case, the shape of the current as a function of eV is determined by the I_{\rightarrow}^{emit} contribution. The PAT current has a natural tendency to decrease when the dot level is raised, however, it displays a step at $\epsilon_D = eV$, provided that $eV < eV_d$. At the step location, the PAT current drops fast, then it decreases more slowly and saturates. The current for large ϵ_D can be thought as a negligible elastic current coming from virtual processes. For $eV > eV_d/2$, if we increase eV , the step height decreases and eventually vanishes when $eV = eV_d$. Hereafter, if one continues to increase eV , the PAT current is still the same as it with $eV = eV_d$ because the energy emission to the mesoscopic device reaches saturation.

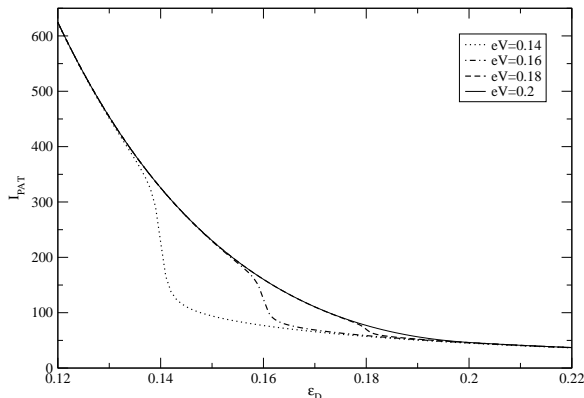


FIG. 6: PAT current depends on dot level ϵ_D with some values of detector bias voltage eV : 0.14, 0.16, 0.18, 0.2 (see legend) at $eV_d = 0.2$.

From this result, we expect that by controlling the detector circuit (varying eV and ϵ_D), we can make a mapping of the spectral density of noise. Here the frequency $\omega = eV_d$ corresponds to the point where the excess noise of the point contact contains a singularity in its derivative. This constitutes an encouraging scenario for detecting specific features in the noise spectrum.

One can also study (not shown) the dependence of the PAT current on the device bias voltage for several values of the detector bias voltage (chosen smaller than ϵ_D in Fig. 5). When $eV_d \ll \epsilon_D$, one gets a current which is independent of eV . This current is identified as a residual elastic current. When $eV_d \gtrsim \epsilon_D$ the PAT current displays a broad maximum, and beyond this the dependence of the PAT current with respect to the detector bias voltage is reversed: the PAT current changes sign. The maximum corresponds to the intensity of noise where the right and the left currents have the same derivative.

V. CONCLUSION

In conclusion, we have considered inelastic Andreev transport in an normal lead/dot/superconductor junction as a probe of high frequency noise. The inelastic contribution to the current flowing in the detector circuit can be thought as a dynamical Coulomb blockade effect where the phase of the junction is related to voltage fluctuations across the dot-superconductor junction. Such voltage fluctuations originate from the current fluctuations in a nearby mesoscopic device. The two types of fluctuations are related by a trans-impedance. This general philosophy was initially proposed in Ref. 10, using a single electron transition. However, here, because of the nature of Andreev transport, two electrons transitions (elastic or inelastic) are required for a current to flow in the detector, which is a novelty of this work.

The tunneling rate is computed in the T-matrix formalism keeping higher order tunneling processes in order to include the Andreev transitions. As the dot level position can be adjusted to filter specific energies, the detector has been shown to isolate noise contributions from both absorption and emission processes. By varying eV or ϵ_D or both, we obtain the signature of noise via the measurement of a DC current in the detector circuit. In particular, we have shown that it is possible to identify the location of the noise derivative singularity with this scheme, by changing the dot level position.

The present proposal has been tested using a quantum point contact as a noise source, because the spectral density of excess noise is well characterized and because it has a simple form. It would be useful to test the present model to situations where the noise spectrum exhibits cusps or singularities. Cusps are known to occur in the high frequency (close to the gap) noise of normal superconducting junctions. Singularities in the noise are known to occur in chiral Luttinger liquid, tested in the context of the fractional quantum Hall effect. Such singularities or cusp should be easy to recognized in the measurement of the photo-assisted current.

Acknowledgments

We thank Richard Deblock and Thibaut Jonckheere for valuable discussions.

VI. APPENDIX A

In this Appendix, we compute the tunneling Hamiltonian operators in the (initial) ground state, which is used in calculations of I_{\leftarrow} .

$$\begin{aligned}
& \langle H_{T1}^+(t-t'_1-t'_2-t'_3+t_1+t_2+t_3)H_{T2}^+(t-t'_2-t'_3+t_1+t_2+t_3)H_{T1}^+(t-t'_3+t_1+t_2+t_3)H_{T2}^+(t+t_1+t_2+t_3) \\
& \times H_{T2}(t_1+t_2+t_3)H_{T1}(t_1+t_2)H_{T2}(t_1)H_{T1}(0) \rangle \\
= & T_1^4 T_2^4 \sum_{k_1 \dots k_4, q_1 \dots q_4, \sigma_1 \dots \sigma_8} \langle c_{q_1 \sigma_1}^+(t-t'_1-t'_2-t'_3+t_1+t_2+t_3)c_{q_2 \sigma_3}^+(t-t'_3+t_1+t_2+t_3)c_{q_3 \sigma_6}(t_1+t_2)c_{q_4 \sigma_8}(0) \rangle \\
& \times \langle c_{k_1 \sigma_2}(t-t'_2-t'_3+t_1+t_2+t_3)c_{k_2 \sigma_4}(t+t_1+t_2+t_3)c_{k_3 \sigma_5}^+(t_1+t_2+t_3)c_{k_4 \sigma_7}^+(t_1) \rangle \\
& \times \langle c_{D \sigma_1}(t-t'_1-t'_2-t'_3+t_1+t_2+t_3)c_{D \sigma_2}^+(t-t'_2-t'_3+t_1+t_2+t_3)c_{D \sigma_3}(t-t'_3+t_1+t_2+t_3)c_{D \sigma_4}^+(t+t_1+t_2+t_3) \rangle \\
& \times \langle c_{D \sigma_5}(t_1+t_2+t_3)c_{D \sigma_6}^+(t_1+t_2)c_{D \sigma_7}(t_1)c_{D \sigma_8}^+(0) \rangle \\
& \times \langle e^{i\phi(t-t'_1-t'_2-t'_3+t_1+t_2+t_3)} e^{i\phi(t-t'_3+t_1+t_2+t_3)} e^{-i\phi(t_1+t_2)} e^{-i\phi(0)} \rangle . \tag{28}
\end{aligned}$$

Simplifications occur because the quantum dot has a singly occupied level with energy ϵ_D . As in Ref. 20, the first electron is transferred to the lead before the second hops on the quantum dot. Therefore,

$$\begin{aligned}
& \langle c_{D \sigma_1}(t-t'_1-t'_2-t'_3+t_1+t_2+t_3)c_{D \sigma_2}^+(t-t'_2-t'_3+t_1+t_2+t_3)c_{D \sigma_3}(t-t'_3+t_1+t_2+t_3)c_{D \sigma_4}^+(t+t_1+t_2+t_3) \rangle \\
& \times \langle c_{D \sigma_5}(t_1+t_2+t_3)c_{D \sigma_6}^+(t_1+t_2)c_{D \sigma_7}(t_1)c_{D \sigma_8}^+(0) \rangle \\
= & \langle c_{D \sigma_1}(t-t'_1-t'_2-t'_3+t_1+t_2+t_3)c_{D \sigma_2}^+(t-t'_2-t'_3+t_1+t_2+t_3) \rangle \langle c_{D \sigma_3}(t-t'_3+t_1+t_2+t_3) \rangle c_{D \sigma_4}^+(t+t_1+t_2+t_3) \rangle \\
& \times \langle c_{D \sigma_5}(t_1+t_2+t_3)c_{D \sigma_6}^+(t_1+t_2) \rangle \langle c_{D \sigma_7}(t_1)c_{D \sigma_8}^+(0) \rangle \\
= & G_{D \sigma_1}(-t'_1)\delta_{\sigma_1 \sigma_2} G_{D \sigma_3}(-t'_3)\delta_{\sigma_3 \sigma_4} G_{D \sigma_5}(t_3)\delta_{\sigma_5 \sigma_6} G_{D \sigma_7}(t_1)\delta_{\sigma_7 \sigma_8} , \tag{29}
\end{aligned}$$

with $G_{D \sigma} \equiv \langle c_{D \sigma}(t)c_{D \sigma}^+(0) \rangle = e^{-i(\epsilon_D - \mu_D)t}$ is the Green's function of QD.

Describing the Andreev process, we assume

$$\begin{aligned}
& \sum_{q_1 \dots q_4} \langle c_{q_1 \sigma_1}^+(t-t'_1-t'_2-t'_3+t_1+t_2+t_3)c_{q_2 \sigma_3}^+(t-t'_3+t_1+t_2+t_3)c_{q_3 \sigma_6}(t_1+t_2)c_{q_4 \sigma_8}(0) \rangle \\
= & \sum_{q_1 \dots q_4} \langle c_{q_1 \sigma_1}^+(t-t'_1-t'_2-t'_3+t_1+t_2+t_3)c_{q_2 \sigma_3}^+(t-t'_3+t_1+t_2+t_3) \rangle \langle c_{q_3 \sigma_6}(t_1+t_2)c_{q_4 \sigma_8}(0) \rangle \\
= & F_{\sigma_1}^*(t'_1+t'_2)\delta_{\sigma_3, -\sigma_1} F_{\sigma_8}(t_1+t_2)\delta_{\sigma_6, -\sigma_8} , \tag{30}
\end{aligned}$$

where $F_{\sigma}(t) \equiv \langle \sum_{qq'} c_{q, -\sigma}(t)c_{q', \sigma}(0) \rangle = \sum_q \text{sgn}(\sigma) u_q v_q e^{-iE_q t}$ is the Green's function of the superconductor with the only notice of Andreev process.

For the correlation of operators in lead, using the Wick's theorem we obtain

$$\begin{aligned}
& \sum_{k_1 \dots k_4} \langle c_{k_1 \sigma_2}(t-t'_2-t'_3+t_1+t_2+t_3)c_{k_2 \sigma_4}(t+t_1+t_2+t_3)c_{k_3 \sigma_5}^+(t_1+t_2+t_3)c_{k_4 \sigma_7}^+(t_1) \rangle \\
= & \sum_{k_1 \dots k_4} [-\langle c_{k_1 \sigma_2}(t-t'_2-t'_3+t_1+t_2+t_3)c_{k_3 \sigma_5}^+(t_1+t_2+t_3) \rangle \langle c_{k_2 \sigma_4}(t+t_1+t_2+t_3)c_{k_4 \sigma_7}^+(t_1) \rangle \\
& + \langle c_{k_1 \sigma_2}(t-t'_2-t'_3+t_1+t_2+t_3)c_{k_4 \sigma_7}^+(t_1) \rangle \langle c_{k_2 \sigma_4}(t+t_1+t_2+t_3)c_{k_3 \sigma_5}^+(t_1+t_2+t_3) \rangle] \\
= & -G_{L \sigma_2}(t-t'_2-t'_3)\delta_{\sigma_2, \sigma_5} G_{L \sigma_4}(t+t_2+t_3)\delta_{\sigma_4, \sigma_7} \\
& + G_{L \sigma_2}(t-t'_2-t'_3+t_2+t_3)\delta_{\sigma_2, \sigma_7} G_{L \sigma_4}(t)\delta_{\sigma_4, \sigma_5} , \tag{31}
\end{aligned}$$

with $G_{L \sigma}(t) \equiv \langle \sum_{k, k'} c_{k \sigma}(t)c_{k' \sigma}^+(0) \rangle = \sum_k e^{-i(\epsilon_k - \mu_L)t}$ is the Green's function of the normal metal lead.

Concerning the phase fluctuations, the four-point correlator which is implicit in the expression of the tunneling current is first written as a time ordered product, then computed using the generalized Wick's theorem. Once ordered, the product of the exponential gives the exponential of the sum of all pairings between phase operators²². As a result, with the definition of Eq. (15), one gets

$$\begin{aligned}
& \langle e^{i\phi(t-t'_1-t'_2-t'_3+t_1+t_2+t_3)} e^{i\phi(t-t'_3+t_1+t_2+t_3)} e^{-i\phi(t_1+t_2)} e^{-i\phi(0)} \rangle \\
= & \frac{e^{J(t-t'_1-t'_2-t'_3+t_1+t_2+t_3)+J(t-t'_3+t_1+t_2+t_3)+J(t-t'_1-t'_2-t'_3+t_3)+J(t-t'_3+t_3)}}{e^{J(-t'_1-t'_2)+J(t_1+t_2)}} . \tag{32}
\end{aligned}$$

The calculation of this for I_{\rightarrow} goes along the same lines. We will omit it here.

VII. APPENDIX B

In this Appendix, we present the denominator products which appear in the tunneling current. Such denominators come from the energy denominators of the transition operator T.

D^0 is the original denominator which is not affected by the environment

$$D^0 = \left\{ \frac{1}{(\epsilon - \epsilon_D - i\eta)(\epsilon - E' - i\eta)(\epsilon_D + E' + i\eta)} \times \left[\frac{1}{(\epsilon - \epsilon_D + i\eta)(\epsilon - E + i\eta)} + \frac{1}{(-\epsilon - \epsilon_D + i\eta)(-\epsilon - E + i\eta)} \right] \frac{1}{(\epsilon_D + E - i\eta)} \right\}^{-1}. \quad (33)$$

D^{el} is the denominator product in the I_{\rightarrow}^{el} which is affected by the environment

$$D^{el} = \left\{ \frac{1}{(\epsilon - \epsilon_D - i\eta)(\epsilon - E' - \omega - i\eta)(\epsilon_D + E' + \omega + i\eta)} \times \left[\frac{1}{(\epsilon - \epsilon_D + i\eta)(\epsilon - E + i\eta)} + \frac{1}{(-\epsilon - \epsilon_D + i\eta)(-\epsilon - E + i\eta)} \right] \frac{1}{(\epsilon_D + E - i\eta)} + \frac{1}{(\epsilon - \epsilon_D - i\eta)(\epsilon - E' - i\eta)(\epsilon_D + E' + i\eta)} \times \left[\frac{1}{(\epsilon - \epsilon_D + i\eta)(\epsilon - E - \omega + i\eta)} + \frac{1}{(-\epsilon - \epsilon_D + i\eta)(-\epsilon - E - \omega + i\eta)} \right] \frac{1}{(\epsilon_D + E + \omega - i\eta)} \right\}^{-1}. \quad (34)$$

D^{inel} is the denominator product attributed to the inelastic current (affected by environment) and it is defined as

$$D^{inel} = \left\{ \frac{1}{(\epsilon_D - \epsilon + i\eta)(\epsilon_D - \epsilon - i\eta)} \left[\frac{1}{(E' + \epsilon_D - \epsilon - \epsilon' + i\eta)(E' - \epsilon + i\eta)} + \frac{1}{(E' + \epsilon_D + i\eta)(E' + \epsilon' + i\eta)} \right] \times \left[\frac{1}{(E + \epsilon_D - \epsilon - \epsilon' - i\eta)(E - \epsilon - i\eta)} + \frac{1}{(E + \epsilon_D - i\eta)(E + \epsilon' - i\eta)} \right] + \frac{1}{(\epsilon_D - \epsilon + i\eta)(\epsilon_D - \epsilon' - i\eta)} \left[\frac{1}{(E' + \epsilon_D - \epsilon - \epsilon' + i\eta)(E' - \epsilon + i\eta)} + \frac{1}{(E' + \epsilon_D + i\eta)(E' + \epsilon' + i\eta)} \right] \times \left[\frac{1}{(E + \epsilon_D - \epsilon - \epsilon' - i\eta)(E - \epsilon' - i\eta)} + \frac{1}{(E + \epsilon_D - i\eta)(E + \epsilon - i\eta)} \right] \right\}^{-1}. \quad (35)$$

-
- ¹ S.R. Eric Yang, Solid State Commun. **81**, 375 (1992).
² Y.M. Blanter and M. Büttiker, Phys. Rep. **336**, 1 (2000).
³ C. Chamon, D. E. Freed, and X. G. Wen, Phys. Rev. B **53**, 4033 (1996).
⁴ T. Martin and R. Landauer, Phys. Rev. B **45**, 1742 (1992); M. Büttiker, Phys. Rev. B **45**, 3807 (1992).
⁵ G. B. Lesovik and R. Loosen, Pis'ma Zh. Éksp. Teor. Fiz. **65**, 280 (1997) [JETP Lett. **65**, 295, (1997)].
⁶ N. M. Chtchelkatchev, G. Blatter, G. B. Lesovik and T. Martin, Phys. Rev. B **66**, 161320(R) (2002).
⁷ A. V. Lebedev, G. B. Lesovik, and G. Blatter, Phys. Rev. B **72**, 245314 (2005).
⁸ A. V. Lebedev, A. Crepieux, and T. Martin Phys. Rev. B **71**, 075416 (2005).
⁹ B. Trauzettel, I. Safi, F. Dolcini, and H. Grabert, Phys. Rev. Lett. **92**, 226405, (2004).
¹⁰ R. Aguado and L. Kouwenhoven, Phys. Rev. Lett. **84**, 1986 (2000).
¹¹ R. Deblock, E. Onac, L. Gurevich, and L. P. Kouwenhoven, Science **301**, 203 (2003).
¹² P.-M. Billangeon, F. Pierre, H. Bouchiat, and R. Deblock, cond-mat/0508676.
¹³ A. Onac, F. Balestro, B. Trauzettel, C. F.J. Lodewijk, and L. Kouwenhoven, Phys. Rev. Lett. **96**, 026803 (2006).
¹⁴ G. E. Blonder, M. Tinkham, and T. M. Klapwijk, Phys. Rev. B **25**, 4515 (1982).
¹⁵ G. L. Ingold and Yu. V. Nazarov, in *Single Charge Tunneling*, H. Grabert and M.H. Devoret eds. (Plenum, New York 1992).
¹⁶ U. Gavish, Y. Levinson, and Y. Imry, Phys. Rev. B. **62**, 637 (2000).
¹⁷ T. Martin in Les Houches Summer School session LXXXI, edited by E. Akkermans, H. Bouchiat, S. Gueron, and G. Montambaux (Elsevier, 2005).
¹⁸ G. Falci, R. Fazio, A. Tagliacozzo, and G. Giaquinta, Europhys. Lett. **30**, 169 (1995).
¹⁹ P. Devillard, R. Guyon, T. Martin, I. Safi, and B. K. Chakraverty, Phys. Rev. B **66**, 165413 (2002).
²⁰ P. Recher, E.V. Sukhorukov, and D. Loss, Phys. Rev. B **63**, 165314 (2001).
²¹ G. B. Lesovik, T. Martin, and G. Blatter, Eur. Phys. J. B **24**, 287 (2001).

- ²² I. Safi, P. Devillard and T. Martin, Phys. Rev. Lett. **86**, 4628 (2001).
- ²³ P. Recher and D. Loss, Phys. Rev. B **65**, 165327 (2002).
- ²⁴ E. Dupont and K. Le Hur, cond-mat/0507282.
- ²⁵ P. Recher, *Correlated Spin Transport in Nanostructures: Entanglement Creation and Spin Filtering*—Ph. D. Thesis, (Sheker Verlag, Aachen, 2004).